One-Step Assembly of Coordination Complexes for Versatile Film and Particle Engineering

Hirotaka Ejima, Joseph J. Richardson, Kang Liang, James P. Best, Martin P. van Koeverden, Georgina K. Such, Jiwei Cui, Frank Caruso*

The development of facile and versatile strategies for thin-film and particle engineering is of immense scientific interest. However, few methods can conformally coat substrates of different composition, size, shape, and structure. We report the one-step coating of various interfaces using coordination complexes of natural polyphenols and Fe(III) ions. Film formation is initiated by the adsorption of the polyphenol and directed by pH-dependent, multivalent coordination bonding. Aqueous deposition is performed on a range of planar as well as inorganic, organic, and biological particle templates, demonstrating an extremely rapid technique for producing structurally diverse, thin films and capsules that can disassemble. The ease, low cost, and scalability of the assembly process, combined with pH responsiveness and negligible cytotoxicity, makes these films potential candidates for biomedical and environmental applications.

Advances in materials design and application are highly dependent on the development of versatile thin-film and particle engineering strategies (*1*–*4*). Supramolecular metal-organic thin films have attracted widespread interest due to their diverse properties, which include (i) stimuli responsiveness imparted by the dynamic nature of supramolecular coordination bonds, (ii) hybrid physicochemical properties of both metals and organic materials, and (iii) controlled structure and functionality achieved by variation of the molecular building blocks (*5*, *6*). Although metal-organic thin films show potential for sensing, separation processes, and catalysis (*5*, *6*), such films are fabricated with multiple, time-consuming steps (*7*–*11*). Moreover, biomedical applications of these films have thus far been limited because they can be toxic or unstable in water (*12*).

We report a simple, rapid, and robust conformal coating method using the one-step assembly of coordination complexes on a range of substrates to prepare various films and particles. The natural polyphenol tannic acid (TA) and Fe^{III} were chosen as the organic ligand and the inorganic cross-linker, respectively. Film deposition occurs upon mixing TA and Fe^{III} in water at ambient temperature. No special equipment is necessary for this method, and the material components are readily available and inexpensive. Moreover, they are generally recognized as safe (GRAS) by the U.S. Food and Drug Administration. Although the chemical structure of TA is usually given as a decagalloyl glucose ($C_{76}H_{52}O_{46}$) (fig. S1) (*13*), it is actually a mixture of polygalloyl glucose molecules with different degrees of esterification (*14*). Three galloyl groups from TA can react with each Fe^{III} ion to form a stable octahedral complex (*15*), allowing each TA molecule to react with several Fe^{III} centers to form a cross-linked film. This method is applicable to a wide variety of substrates because of the general surface binding affinity of TA. When these films are deposited on particles, subsequent dissolution of the templates results in the formation of three-dimensional free-standing films known as hollow capsules. Such systems have widespread use in drug and gene delivery, catalysis, and biosensing; they can also function as microreactors (*16*).

We first describe the deposition of Fe^{III}-TA films on planar (Fig. 1A) and particulate (Fig. 1, B to K) polystyrene (PS) templates. The color of the template suspension immediately turned blue upon addition of Fe^{III} and TA solutions (fig. S2). Stirring times (20 s and 1 hour) had no effect on the color or on the resulting film thickness under standard conditions (*13*), implying that the film formation process was completed instantaneously. Formation of the Fe^{III}-TA films on the PS particles shifted the surface zeta potential from –27 ± 3 mV to –64 ± 7 mV because of the acidic nature of the galloyl groups in TA. After removing the PS template, we obtained highly uniform microcapsules with a zeta potential of –65 ± 7 mV, which was within error the same value as before template removal.

Differential interference contrast (DIC) microscopy, atomic force microscopy (AFM), scanning electron microscopy (SEM), and transmission electron microscopy (TEM) images of the Fe^{III}-TA capsules obtained from D = 3.6 μm templates are shown in Fig. 1, B to E. Monodisperse, spherical capsules were readily observed under DIC (Fig. 1B). The permeability of these capsules is molecular weight–dependent and they are essentially impermeable to 2000-kD dextran (fig. S3).

Department of Chemical and Biomolecular Engineering, The University of Melbourne, Parkville, Victoria 3010, Australia.
*Corresponding author. E-mail: fcaruso@unimelb.edu.au

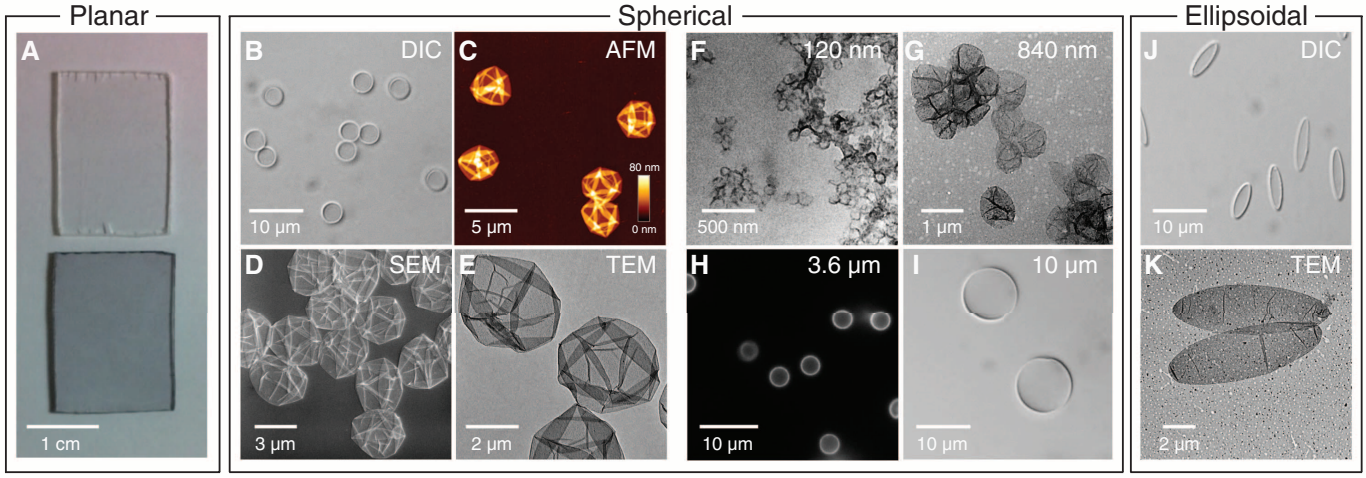

Fig. 1. Film formation. Fe^{III}-TA films prepared on PS substrates with various shapes (planar, spherical, and ellipsoidal) and sizes (D = 120 nm to 10 μm). (**A**) Photograph of PS slides before (top) and after (bottom) Fe^{III}-TA coating. (**B** to **K**) Microscopy images of Fe^{III}-TA capsules: DIC images [(B), (I), and (J)], AFM images (C), TEM images [(E), (F), (G), and (K)], SEM image (D), and fluorescence microscopy image (H).

The presence of Fe in the films was confirmed by energy-dispersive x-ray spectroscopy (EDS) (fig. S4) and x-ray photoelectron spectroscopy (XPS) (fig. S5). The capsules observed by AFM, SEM, and TEM (Fig. 1, C to E) had folds and creases because these measurements were performed on dried samples. Different-sized templates (D = 120 nm, 840 nm, 3.6 μm, and 10 μm) can be exploited for capsule preparation (Fig. 1, F to I). Ellipsoidal PS templates, prepared by stretching spherical PS particles above their glass transition temperature, were also used to obtain ellipsoidal capsules (Fig. 1, J and K). From AFM height analysis, the single-wall thickness of the capsules was determined to be half the minimum height of the collapsed flat regions (10.4 ± 0.6 nm). The Young's modulus (E_Y) of the D = 3.6 μm PS-templated capsules was estimated to be 1.0 ± 0.2 GPa by AFM force measurements (fig. S6). This value of E_Y is at the high end of the range observed for layer-by-layer (LbL) polyelectrolyte capsules (10 to 1000 MPa) (*17*). Several groups have reported LbL capsules fabricated from TA and other polymers (*18*, *19*). For example, LbL capsules of TA-poly(*N*-vinylpyrrolidone) (PVPON) exhibit a bilayer thickness of 1.0 to 2.2 nm, depending on the molecular weight of the PVPON (*19*). The Fe^{III}-TA film obtained through one-step assembly is thicker than four bilayers of TA-PVPON obtained through multistep LbL assembly, demonstrating the efficiency of the one-step process. Analogous to LbL assembly, the thickness of Fe^{III}-TA films can be further increased by simply repeating the rapid coating procedure (figs. S7 and S8).

The effect of TA and $FeCl_3{\cdot}6H_2O$ concentrations (hereafter denoted [TA] and [$FeCl_3{\cdot}6H_2O$], respectively) on the resulting film thickness and morphology were investigated by AFM using D = 3.6 μm PS-templated capsules. When [TA] was kept constant at 0.40 mg ml^{-1} (0.24 mM), capsules were obtained over a [$FeCl_3{\cdot}6H_2O$] range of 0.06 to 0.20 mg ml^{-1} (0.22 to 0.74 mM), approximately corresponding to molar ratios of 1:1 to 3:1 between Fe^{III} and TA. The resulting stoichiometries in the capsule walls were determined by XPS (fig. S5) to be Fe^{III}:TA ≈ 1:4, 1:3, and 1:2 for feed [$FeCl_3{\cdot}6H_2O$] of 0.06, 0.12, and 0.20 mg ml^{-1}, respectively. This demonstrates that the feed concentrations influence the capsule stoichiometries. Above and below [$FeCl_3{\cdot}6H_2O$] = 0.06 to 0.20 mg ml^{-1}, aggregated capsules and few capsules were formed, respectively. In the absence of Fe^{III}, no capsules were formed. As [$FeCl_3{\cdot}6H_2O$] was increased in this concentration range, the thickness of the Fe^{III}-TA film increased from 7.7 ± 0.4 nm to 11.9 ± 1.2 nm and exhibited increased roughness (fig. S9). Increasing the amount of Fe^{III} to three molar equivalents of TA resulted in capsules that had a grainy surface because of the excess Fe^{III} (fig. S9A). Values of root-mean-square roughness (300 nm × 300 nm, fold-free flat region) were 1.3 ± 0.1 nm, 1.6 ± 0.1 nm, and 7.7 ± 0.4 nm for [$FeCl_3{\cdot}6H_2O$] of 0.06, 0.10, and 0.20 mg ml^{-1}, respectively. In contrast to these observations based on Fe^{III}, [TA] had minimal impact upon film assembly. Capsules with constant film thickness and roughness were obtained throughout a concentration range of [TA] = 0.10 to 1.80 mg ml^{-1} (0.06 to 1.06 mM) when [$FeCl_3{\cdot}6H_2O$] was fixed at 0.10 mg ml^{-1} (0.37 mM) (fig. S10). These results suggest that TA was relatively in higher excess than Fe^{III} under these conditions, and that Fe^{III}, not TA, influenced the film thickness.

To further investigate the mechanism of the Fe^{III}-TA film formation, we used polyethyleneimine (PEI)–coated PS templates for capsule preparation. The PEI coating changed the zeta potential of the templates from negative (–27 ± 3 mV) to positive (37 ± 6 mV). Capsules were still formed with these positively charged templates, indicating that the surface charge is not an important factor for film deposition. We also determined the zeta potential after incubating the bare PS particles with either TA or $FeCl_3$. The adsorption of TA reduced the zeta potential to –39 ± 4 mV, whereas the value was slightly changed after incubation with $FeCl_3$ (–33 ± 5 mV). Rapid surface adherence and formation of a TA layer on the template particle surface were confirmed by adsorption experiments (fig. S11). Catechol-functionalized molecules and their derivatives have a high affinity for a wide variety of substrates with different surface charges (*4*, *20*). Thus, it is most likely that the free TA or small Fe^{III}-TA complexes initially adsorb onto the template surface and are subsequently cross-linked by further Fe^{III} complexation. The increase in the cross-linker concentration causes the attraction of more TA to the initially formed films, making them thicker. Film growth is completed when free Fe^{III} in the bulk solution is consumed. Excess Fe^{III} induces aggregation of Fe^{III}-TA complexes in the bulk solution. These small aggregates subsequently bind to the surface, leading to an increased roughness of the capsule films (fig. S12). Unlike thin-film formation using dopamine self-polymerization (*4*), this study relies on the complexation of TA with Fe^{III} through coordination bonds, which allows the films to form rapidly and disassemble in response to pH (see below).

To show the versatility of this method, we coated various planar and particulate substrates exhibiting different surface properties (anionic,

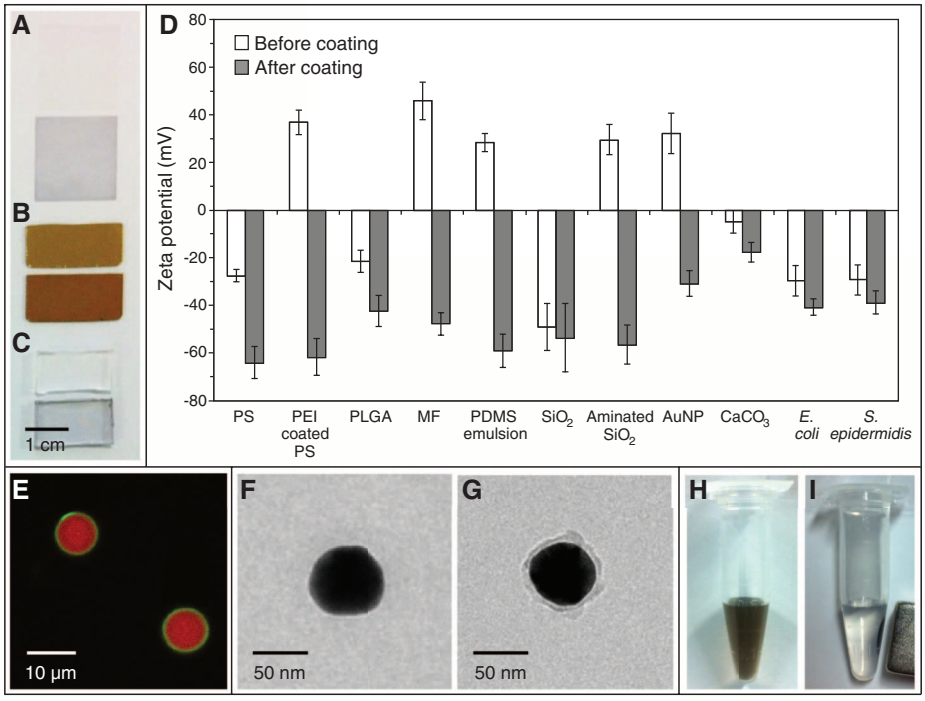

Fig. 2. Fe^{III}-TA coating on various substrates. (**A** to **C**) Photograph of planar substrates before (upper) and after (lower) Fe^{III}-TA coating: glass (A), Au (B), and PDMS (C). (**D**) Zeta potential values of particulate substrates in water before and after Fe^{III}-TA coating. Data are means ± SD. (**E**) Confocal laser scanning microscopy image of protein-loaded $CaCO_3$ particles (red) coated with Fe^{III}-TA films (green). (**F** and **G**) TEM images of Au NPs noncoated (F) and coated (G) with a Fe^{III}-TA film. (**H** and **I**) Photographs of Fe^{III}-TA capsules loaded with Fe_3O_4 nanoparticles dispersed in water before (H) and after (I) applying a magnet.

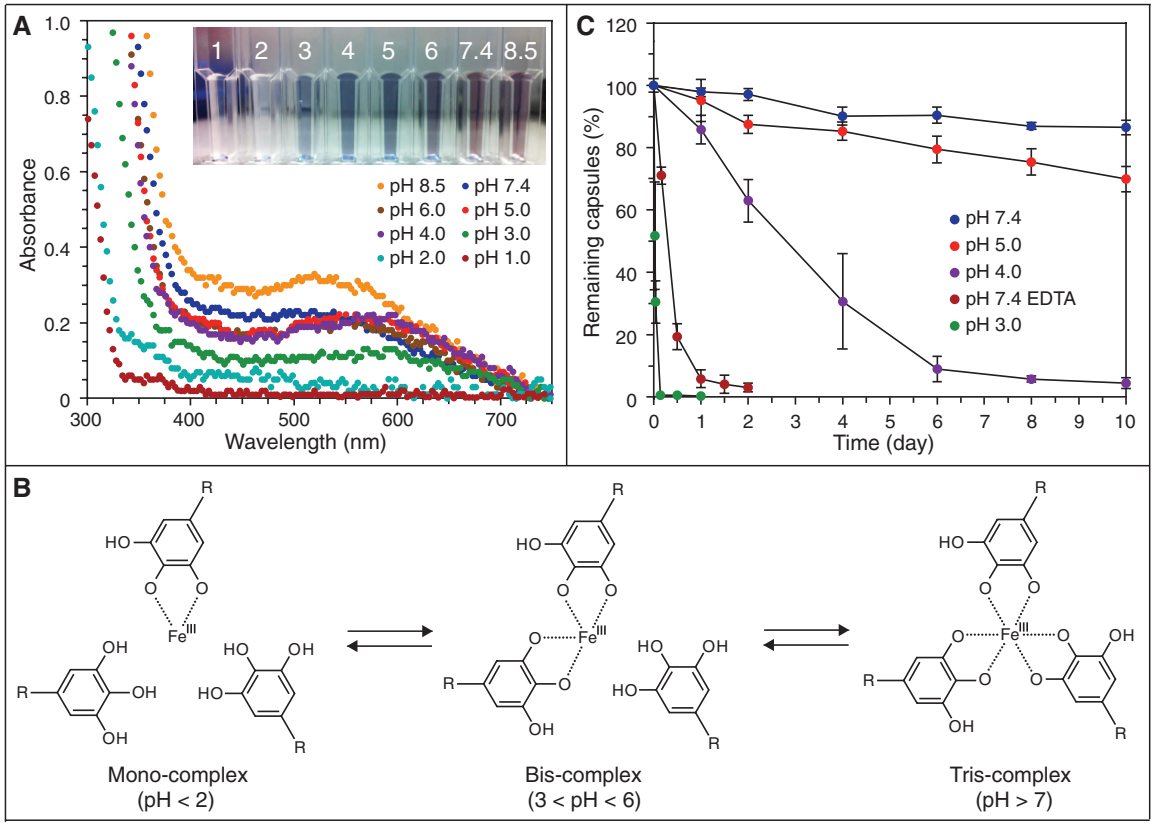

Fig. 3. pH-responsive disassembly of Fe^{III}-TA capsules. (**A**) Ultraviolet to visible absorption spectra of spherical Fe^{III}-TA capsule dispersions (D = 3.6 μm, 4.0 × 10^7 capsules ml^{-1}) at various pH values. Inset is a photograph of the capsule dispersions at the indicated pH values. (**B**) pH-dependent transition of dominant Fe^{III}-TA complexation state. R represents the remainder of the TA molecule. (**C**) Plot of remaining capsule population versus time. Data are means ± SD from three independent measurements.

neutral, and cationic)—including glass, gold (Au), polydimethylsiloxane (PDMS), poly(lactic-*co*-glycolic acid) (PLGA), melamine-formaldehyde resin, low–molecular weight PDMS emulsion, silica (SiO_2), aminated SiO_2, cetyltrimethylammonium bromide–capped Au nanoparticles (Au NPs), calcium carbonate ($CaCO_3$), *Escherichia coli*, and *Staphylococcus epidermidis*—with the Fe^{III}-TA films (Fig. 2). The color and zeta potential values (Fig. 2, A to D) changed after the coating in all cases, demonstrating that Fe^{III}-TA films can be formed on a wide variety of substrates. Figure 2E and fig. S13A show protein- and rhodamine B–loaded $CaCO_3$ coated with Fe^{III}-TA films, respectively. Replica particles were obtained by filling mesoporous $CaCO_3$ particles with Fe^{III}-TA complexes and dissolving the $CaCO_3$ cores (fig. S13, B to E). After the coating, a Fe^{III}-TA shell layer was visible around the Au NP core (Fig. 2, F and G, and fig. S13F). Magnetic Fe_3O_4 nanoparticles were encapsulated by coating low–molecular weight PDMS emulsion templates loaded with Fe_3O_4 nanoparticles (fig. S13G). Subsequent removal of the emulsion by ethanol produced magnetically active Fe^{III}-TA capsules (Fig. 2, H and I).

The coordination between Fe^{III} and TA is pH-dependent, and the obtained capsules exhibit pH-dependent disassembly. The color of the capsule suspension was also pH-dependent (Fig. 3A). The suspension was colorless at pH < 2, blue at 3 < pH < 6, and red at pH > 7. This color change is consistent with observations for analogous Fe^{III}-catechol complexes (*21*, *22*), which can be attributed to transitions between mono-, bis-, and tris-complex states (Fig. 3B). At pH 2.0, the Fe^{III}-TA capsules shrank immediately (fig. S14) and disassembled. At low pH, most of the hydroxyl groups were protonated, which led to rapid destabilization of cross-links and disassembly of the films. Even above pH 3.0, Fe^{III}-TA capsules disassembled. Figure 3C shows the disassembly kinetics of the Fe^{III}-TA capsules. At pH 3.0, all of the capsules had disassembled in 4 hours, whereas at pH 4.0, 6 days of incubation were required to disassemble the majority of the capsules. In contrast, ~70 and 90% of the capsules still remained intact after 10 days of incubation at pH 5.0 and pH 7.4, respectively. The stability constants of Fe^{III}-TA are 1.5 × 10^5, 3.4 × 10^9, and 2.8 × 10^{17} at pH 2, 5, and 8, respectively (*23*). Additionally, we carried out AFM experiments after incubation at pH 5.0 (fig. S15). The films became thinner (6.0 ± 1.4 nm) and rougher, confirming the gradual disassembly of the Fe^{III}-TA films. Ethylenediaminetetraacetic acid (EDTA) accelerated the disassembly because of its strong affinity for Fe^{III} (Fig. 3C).

The cytotoxicity of Fe^{III}-TA capsules was found to be negligible (fig. S16). Coupled with their pH-sensitive disassembly profile, Fe^{III}-TA capsules have potential biomedical application because of the varying pH in different parts of the body [e.g., blood (pH 7.4), stomach (pH 1.0 to 3.0), duodenum (pH 4.8 to 8.2), etc.] (*24*). Iron tannate has been historically recognized as an ink (*25*) and a corrosion-resistant layer for steel (*15*). It had also been used for dyeing teeth black, and consequently preventing cavities, in the old Japanese custom called *ohaguro* (*26*). The general applicability of this technique was further demonstrated by using different metals and another polyphenol (figs. S17 and S18). The simple preparation and biologically tunable physicochemical properties of the metal-polyphenol films provide a platform for the engineering and assembly of advanced materials for potential use in a range of applications.

References and Notes

1. G. Decher, *Science* **277**, 1232–1237 (1997).
2. F. Caruso, R. A. Caruso, H. Möhwald, *Science* **282**, 1111–1114 (1998).
3. D. Y. Ryu, K. Shin, E. Drockenmuller, C. J. Hawker, T. P. Russell, *Science* **308**, 236–239 (2005).
4. H. Lee, S. M. Dellatore, W. M. Miller, P. B. Messersmith, *Science* **318**, 426–430 (2007).
5. A. Bétard, R. A. Fischer, *Chem. Rev.* **112**, 1055–1083 (2012).
6. Y. Yan, J. B. Huang, *Coord. Chem. Rev.* **254**, 1072–1080 (2010).
7. A. Hatzor *et al.*, *J. Am. Chem. Soc.* **120**, 13469–13477 (1998).
8. M. Wanunu *et al.*, *J. Am. Chem. Soc.* **127**, 17877–17887 (2005).
9. R. Kaminker *et al.*, *J. Am. Chem. Soc.* **132**, 14554–14561 (2010).
10. L. Motiei *et al.*, *Langmuir* **27**, 1319–1325 (2011).
11. R. Makiura *et al.*, *Nat. Mater.* **9**, 565–571 (2010).
12. M. Hanke *et al.*, *Langmuir* **28**, 6877–6884 (2012).
13. See supplementary materials on *Science* Online.
14. T. Mori *et al.*, *J. Biol. Chem.* **287**, 6912–6927 (2012).

15. T. K. Ross, R. A. Francis, *Corros. Sci.* **18**, 351–361 (1978).
16. W. Tong, X. Song, C. Gao, *Chem. Soc. Rev.* **41**, 6103–6124 (2012).
17. O. I. Vinogradova, O. V. Lebedeva, B. S. Kim, *Annu. Rev. Mater. Res.* **36**, 143–178 (2006).
18. T. Shutava, M. Prouty, D. Kommireddy, Y. Lvov, *Macromolecules* **38**, 2850–2858 (2005).
19. V. Kozlovskaya, E. Kharlampieva, I. Drachuk, D. Cheng, V. V. Tsukruk, *Soft Matter* **6**, 3596–3608 (2010).
20. Q. Ye, F. Zhou, W. M. Liu, *Chem. Soc. Rev.* **40**, 4244–4258 (2011).
21. H. Xu *et al.*, *ACS Macro Lett.* **1**, 457–460 (2012).
22. N. Holten-Andersen *et al.*, *Proc. Natl. Acad. Sci. U.S.A.* **108**, 2651–2655 (2011).
23. S. Sungur, A. Uzar, *Spectrochim. Acta A* **69**, 225–229 (2008).
24. D. Schmaljohann, *Adv. Drug Deliv. Rev.* **58**, 1655–1670 (2006).
25. V. Rouchon *et al.*, *Anal. Chem.* **83**, 2589–2597 (2011).
26. Y. Tanizawa, K. Sawamura, T. Suzuki, *J. Chem. Soc. Faraday Trans.* **86**, 1071–1075 (1990).

Acknowledgments: Supported by the Australian Research Council under Federation Fellowship FF0776078 (F.C.), Australian Laureate Fellowship FL120100030 (F.C.), Discovery Project DP0877360 (F.C.), Future Fellowship FT120100564 (G.K.S.), and Super Science Fellowship FS110200025 (J.C. and F.C.) schemes. H.E. thanks the Japan Society for the Promotion of Science (JSPS) for a postdoctoral fellowship for research abroad. The data presented in this paper are given in the main text and in the supplementary materials. We thank X. Duan (Surface and Chemical Analysis Network, the University of Melbourne) for assistance with XPS analysis. The University of Melbourne has filed a provisional patent on the assembly process.

Supplementary Materials

www.sciencemag.org/cgi/content/full/341/6142/154/DC1
Materials and Methods
Figs. S1 to S18
References (*27–30*)

1 March 2013; accepted 5 June 2013
10.1126/science.1237265

Nanoscale Atoms in Solid-State Chemistry

Xavier Roy,[1] Chul-Ho Lee,[1,2] Andrew C. Crowther,[3] Christine L. Schenck,[1] Tiglet Besara,[4] Roger A. Lalancette,[6] Theo Siegrist,[4,5] Peter W. Stephens,[7] Louis E. Brus,[1] Philip Kim,[2] Michael L. Steigerwald,[1]* Colin Nuckolls[1]*

We describe a solid-state material formed from binary assembly of atomically precise molecular clusters. $[Co_6Se_8(PEt_3)_6][C_{60}]_2$ and $[Cr_6Te_8(PEt_3)_6][C_{60}]_2$ assembled into a superatomic relative of the cadmium iodide (CdI_2) structure type. These solid-state materials showed activated electronic transport with activation energies of 100 to 150 millielectron volts. The more reducing cluster $Ni_9Te_6(PEt_3)_8$ transferred more charge to the fullerene and formed a rock-salt–related structure. In this material, the constituent clusters are able to interact electronically to produce a magnetically ordered phase at low temperature, akin to atoms in a solid-state compound.

Conventional binary solid-state compounds, A_xB_y, are infinite, crystalline arrays of atoms A and B. Here, we describe analogous binary solids in which the "atomic" building blocks are pseudo-spherical molecular clusters rather than simply atoms [for reviews on molecular clusters, see (*1–3*)]. We prepare these new solids by combining independently synthesized molecular clusters (*4–6*). The internal structures of the constituent clusters remain unchanged, but charge is transferred between them, forming ionic solids analogous to NaCl. We report three new solids: $[Co_6Se_8(PEt_3)_6][C_{60}]_2$, $[Cr_6Te_8(PEt_3)_6][C_{60}]_2$, and $[Ni_9Te_6(PEt_3)_8][C_{60}]$. The former two assemble into a superatomic relative of the CdI_2 structure type, and the latter forms a simple rock-salt crystal.

Despite their ready availability, molecular clusters have been used infrequently as electronic materials. Noteworthy examples of success in this area are the organic-inorganic hybrid materials reported by Batail and Mitzi (*7–11*). Nanocrystals have been assembled into striking superlattices (*12–14*), but they do not have discrete structural, electronic, and magnetic properties and cannot be regarded as genuine artificial atoms. Here, we combine independently prepared electronically and structurally complementary molecular cluster building blocks to form atomically precise binary solid-state compounds. When the building blocks are atoms (ions), binary solids assemble into simple crystalline arrays such as the rock-salt and CdI_2 lattices [for an authoritative text on solid-state inorganic chemistry, see (*15*)]. We show that when similarly sized clusters combine, the same lattice results, albeit at the dramatically increased length scale of nanometers rather than Ångstroms. The constituent clusters interact to produce collective properties such as electrically conducting networks and magnetic ordering.

Our strategy was to use constituent molecular clusters that have the same, roughly spherical, shape but very different electronic properties to encourage reaction and subsequent structural

[1]Department of Chemistry, Columbia University, New York, NY 10027, USA. [2]Department of Physics, Columbia University, New York, NY 10027, USA. [3]Department of Chemistry, Barnard College, New York, NY 10027, USA. [4]National High Magnetic Field Laboratory (NHMFL), Florida State University (FSU), Tallahassee, FL 32310, USA. [5]Department of Chemical and Biomedical Engineering, Florida A&M University–FSU College of Engineering, Tallahassee, FL 32310, USA. [6]Department of Chemistry, Rutgers State University, Newark, NJ 07102, USA. [7]Department of Physics and Astronomy, State University of New York–Stony Brook, Stony Brook, NY 11794, USA.

*Corresponding author. E-mail: cn37@columbia.edu (C.N.); mls2064@columbia.edu (M.L.S.)

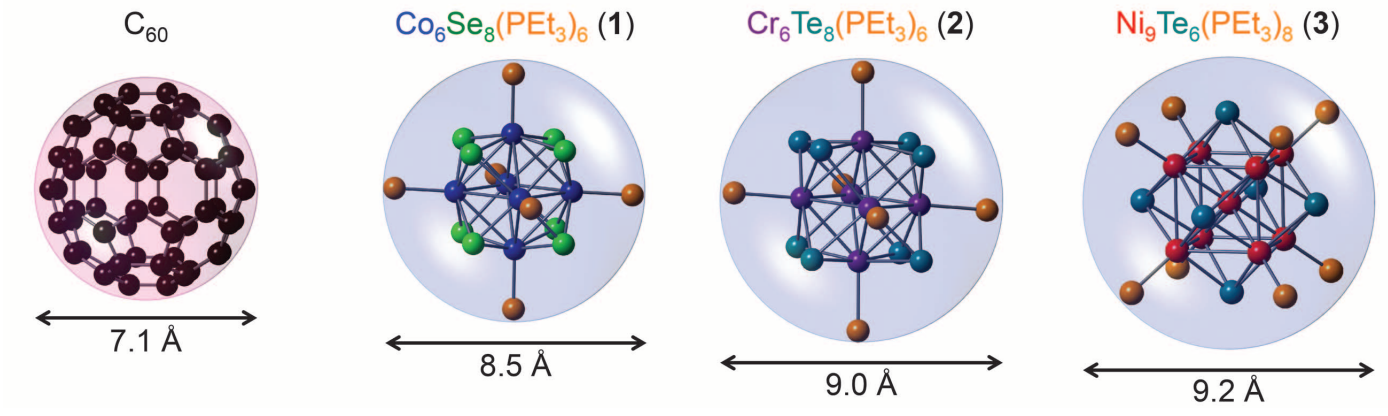

Fig. 1. Structures of the nanoscale atoms as measured by SCXRD. In the figure, the clusters are depicted on the same size scale. The diameter of the cluster is determined as the long diagonal P-P distance. The ethyl groups on the phosphines of **1**, **2**, and **3** were removed to clarify the view.

Science

One-Step Assembly of Coordination Complexes for Versatile Film and Particle Engineering

Hirotaka Ejima, Joseph J. Richardson, Kang Liang, James P. Best, Martin P. van Koeverden, Georgina K. Such, Jiwei Cui and Frank Caruso

Science **341** (6142), 154-157.
DOI: 10.1126/science.1237265

One-Step Coverage

Controllable formation of thin films often requires slow deposition conditions or multiple rounds of coating. **Ejima *et al.*** (p. 154; see the Perspective by **Bentley and Payne**) report a simple and versatile method for coating surfaces with thin biocompatible films made from the condensation of Fe^{3+} ions and a natural polyphenol, tannic acid, from aqueous solutions. Flat surfaces, colloidal particles, and even bacterial cells could be coated, and the coats could subsequently be degraded by changing the pH.

Science (print ISSN 0036-8075; online ISSN 1095-9203) is published by the American Association for the Advancement of Science, 1200 New York Avenue NW, Washington, DC 20005.